

ORIGINAL ARTICLE

Contribution of vascular endothelial growth factor receptor-2 sialylation to the process of angiogenesis

P Chiodelli¹, S Rezzola¹, C Urbinati¹, F Federici Signori¹, E Monti², R Ronca¹, M Presta¹ and M Rusnati¹

Vascular endothelial growth factor receptor-2 (VEGFR2) is the main pro-angiogenic receptor expressed by endothelial cells (ECs). Using surface plasmon resonance, immunoprecipitation, enzymatic digestion, immunofluorescence and cross-linking experiments with specific sugar-binding lectins, we demonstrated that VEGFR2 bears both α ,1-fucose and α (2,6)-linked sialic acid (NeuAc). However, only the latter is required for VEGF binding to VEGFR2 and consequent VEGF-dependent VEGFR2 activation and mitogenic response in ECs. Notably, downregulation of β -galactoside α (2,6)-sialyltransferase expression by short hairpin RNA transduction inhibits VEGFR2 α (2,6) sialylation that is paralleled by an increase of β -galactoside α (2,3)-sialyltransferase expression. This results in an *ex-novo* α (2,3)-NeuAc sialylation of the receptor that functionally replaces the lacking α (2,6)-NeuAc, thus allowing VEGF/VEGFR2 interaction. In keeping with the role of VEGFR2 sialylation in angiogenesis, the α (2,6)-NeuAc-binding lectin *Sambucus nigra* (SNA) prevents VEGF-dependent VEGFR2 autophosphorylation and EC motility, proliferation and mitogenesis. In addition, SNA exerts a VEGF-antagonist activity in tridimensional angiogenesis models *in vitro* and in the chick-embryo chorioallantoic membrane neovascularization assay and mouse matrigel plug assay *in vivo*. In conclusion, VEGFR2-associated NeuAc plays an important role in modulating VEGF/VEGFR2 interaction, EC pro-angiogenic activation and neovessel formation. VEGFR2 sialylation may represent a target for the treatment of angiogenesis-dependent diseases.

Oncogene (2017) 36, 6531–6541; doi:10.1038/onc.2017.243; published online 7 August 2017

INTRODUCTION

Angiogenesis, the formation of new blood vessel from pre-existing ones, plays a key role in different physiological and pathological settings, including embryonic development, inflammation, wound repair, tumor growth and metastasization.¹ At the molecular level, neovascularization results from the interactions of angiogenic growth factors with tyrosine kinase receptors, complex lipids and sugars present in the extracellular milieu or exposed on the endothelial cell (EC) surface. In particular, variations in the EC glycophenotype may modulate angiogenesis by displaying or masking binding sites for pro- or antiangiogenic factors, thus translating glycan composition into functional responses.²

Vascular endothelial growth factors (VEGFs) play a pivotal role in mediating the angiogenic response in several physiological and pathological processes.³ VEGF family comprises six subgroups: VEGF-A, -B, -C, -D, -E and placental growth factor (PlGF), with VEGF-A representing the most important member involved in angiogenesis. Different isoforms of VEGF-A exist, composed of 121, 165, 189, and 206 amino acids. Only the two shorter forms are efficiently secreted, thus representing the most important angiogenic stimuli. VEGF-A₁₆₅ (hereafter abbreviated in VEGF), but not VEGF-A₁₂₁, possess a cationic heparin-binding domain⁴ required for the binding of the growth factor to heparan sulfate proteoglycans (HSPGs) that, together with $\alpha_v\beta_3$ integrin⁵ and neuropilin-1,⁶ act as VEGF-coreceptors.

The primary pro-angiogenic receptors for VEGFs are represented by three distinct tyrosine kinase receptors: VEGFR1 (flt-1), VEGFR2 (KDR) and VEGFR3, among which VEGFR2 (KDR) is the most important mediator of VEGF-A angiogenic activity. VEGFR1 is

also able to bind to VEGF-A, while VEGFR3 preferentially binds to VEGF-C and VEGF-D and is mainly implicated in lymphangiogenesis.⁷

The extracellular region of VEGFR2, composed of 762 amino acids folded into seven immunoglobulin domains,⁸ harbors several N-linked glycosylation sites. VEGFR2 glycosylation is necessary for receptor stability, exposure on the cell surface^{9,10} and even for its activation upon VEGF binding.^{11,12} However, the molecular mechanism(s) linking the glycan moiety of VEGFR2 to its pro-angiogenic activity have not been fully elucidated. Relevant to this point, a direct binding of glycan-binding proteins galectin-1 and -3 to complex N-glycans on VEGFR2 are required to activate a VEGF-like signaling.^{13,14}

Various glycans are associated to cell-surface receptors. Among these, sialic acid (NeuAc) encompasses a large family of sugars characterized by a nine-carbon acidic sugar found mainly as terminal component of glycoproteins where it regulates various molecular interactions.¹⁵ Many observations suggest a possible involvement of NeuAc in VEGFR2 pro-angiogenic activity: it is the major surface anion on ECs,^{16,17} whose expression is regulated during neovascularization.¹⁸ Also, NeuAc linked to glycosylated receptors participates to EC activation induced by platelet endothelial cell adhesion molecule,¹⁹ galectin-1¹⁴ and HIV-1 Tat.²⁰ More to the point, NeuAc is found associated to VEGFR2 glycans¹⁴ and itraconazole inhibits VEGFR2 glycosylation and signaling in ECs.¹⁰ Accordingly, lithocholic acid analogs, that act as sialyltransferase (ST) inhibitors, inhibit angiogenesis in human umbilical vein ECs (HUVECs).²¹ Finally, it is interesting to note that high-molecular-weight VEGF isoforms (including

¹Units of Experimental Oncology and Immunology, University of Brescia, Brescia, Italy and ²Units of Biotechnology, Department of Molecular and Translational Medicine, University of Brescia, Brescia, Italy. Correspondence: Dr P Chiodelli or Professor M Rusnati, Experimental Oncology and Immunology, Department of Molecular and Translational Medicine, viale Europa 11, 25123 Brescia, Italy.

E-mail: paola.chiodelli@unibs.it or marco.rusnati@unibs.it

Received 14 December 2016; revised 30 May 2017; accepted 12 June 2017; published online 7 August 2017

VEGF₁₆₅) possess a cationic domain necessary for the binding to polyanionic HSPGs,²² inferring the possibility that the same domain mediates VEGF₁₆₅ binding to anionic NeuAc residues of VEGFR2.

Taken together, these evidences prompted us to demonstrate the association of NeuAc to VEGFR2 and its role in mediating the binding of the receptor to VEGF and in inducing EC pro-angiogenic activation.

RESULTS

VEGFR2 glycosylation

Lectins with specific sugar-binding capacity are a valuable tool for the characterization of the cell glycophenotype.²³ Also, surface plasmon resonance (SPR) analysis represents an efficient technique to investigate lectin-sugar interactions.²⁴ Thus, in order to get novel insights about VEGFR2 glycosylation, different lectins (Table 1) were assessed for their capacity to bind to the extracellular moiety of VEGFR2 (VEGFR2-Fc) when immobilized to a SPR sensorchip.

In preliminary experiments, fully glycosylated VEGFR2-Fc purified from murine myeloma cells was immobilized to a SPR sensorchip and evaluated for its capacity to interact with its physiological ligand VEGF. As shown in Figure 1 (upper panels), VEGF binds to the immobilized receptor in a dose-dependent and saturable manner (Table 1), indicating that VEGFR2 retains its binding capability after immobilization.

On this basis, a series of sugar-binding lectins were analyzed for their capacity to interact with immobilized VEGFR2: L-PHA, that recognizes complex type N-glycans containing a β 1,6-linked branch to which both fucose and NeuAc are attached;²⁵ UEA-1, that recognizes terminal fucose residues;²⁶ SNA and MAA, that recognize terminal NeuAc linked to α (2,6)- and α (2,3)-NeuAc, respectively.^{27,28} As shown in Figure 1 and Table 1, SNA and UEA-1 bind to immobilized VEGFR2-Fc in a dose-dependent and saturable manner whereas L-PHA/VEGFR2-Fc interaction does not reach saturation at the concentrations tested. Noticeably, MAA, that binds NeuAc residues with a different glycosidic bond when compared to SNA, shows a very limited capacity to interact with immobilized VEGFR2.

In conclusion, by using sugar-binding lectins was possible to demonstrate that both fucose and α (2,6)- but not α (2,3)-NeuAc are linked to glycans of VEGFR2 purified from murine myeloma cells.

Since dramatic changes in glycosylation pattern can occur among individual cell types,²⁹ we investigated the association of NeuAc and fucose to VEGFR2 directly at the surface of ECs. Firstly, the total extent of VEGFR2 glycosylation was assessed by treating HUVECs with tunicamycin, in order to block protein N-glycosylation. This was followed by cell-surface biotinylation and

immunoprecipitation with anti-VEGFR2 antibody. As shown in Figure 2a, the mature form of VEGFR2 is characterized by an apparent molecular weight (MW) of 250 kDa. Treatment with tunicamycin causes the accumulation of a low MW 150 kDa receptor at the surface of HUVECs, indicating that it inhibits VEGFR2 glycosylation without interfering with the intracellular trafficking and surface expression of the receptor.

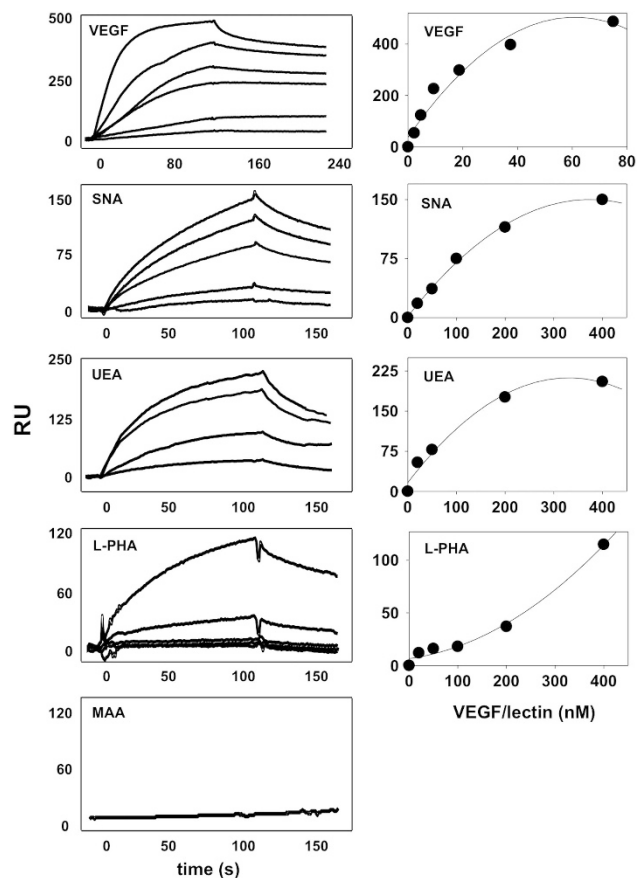


Figure 1. SPR analysis of the interaction of VEGFR2 with VEGF or lectins. Left panels: representative blank subtracted sensorgram overlays resulting from the injection of increasing concentrations of VEGF (2.5, 5, 10, 20, 40, 80 nM) or of the different lectins (25, 50, 100, 200, 400 nM) onto sensorchip-immobilized VEGFR2. Right panels: steady-state analysis obtained by fitting the proper form of Scatchard's equation for the plot of the bound RU at equilibrium versus the concentration of VEGF or of lectins in solution.

Table 1. Binding parameters of the interaction of lectins or of VEGF to sensorchip-immobilized VEGFR2

Lectin	(MW)	Sugar residues specificity	K_d (nM)	
			kinetic	equilibrium
SNA	(140)	Neu5Ac α 6Gal(NAc)	135	110
MAA	(130)	Neu5Ac/Gc α 3Gal β 4GlcNAc	ND	ND
UEA-1	(63)	α Fuc	316	140
L-PHA	(126)	Gal β 4GlcNAc β 6(GlcNAc β 2Man α 3)Man α 3	633	> 400
GSL-IB ₄	(113)	α Gal	Not analyzed	Not analyzed
LEL	(71)	(GlcNAc) ₂₋₄	Not analyzed	Not analyzed
ECL	(54)	Gal β 4GlcNAc	Not analyzed	Not analyzed
VEGF			19.8	18.0

K_d values were either derived from the association/dissociation constants ratio (kinetic) or by Scatchard plot analysis of the equilibrium binding data. The results shown are representative of two other experiments that gave similar results. ND, not determinable. The molecular weight (MW, in kDa) of the various lectins and the specific sugar residues recognized are also reported.

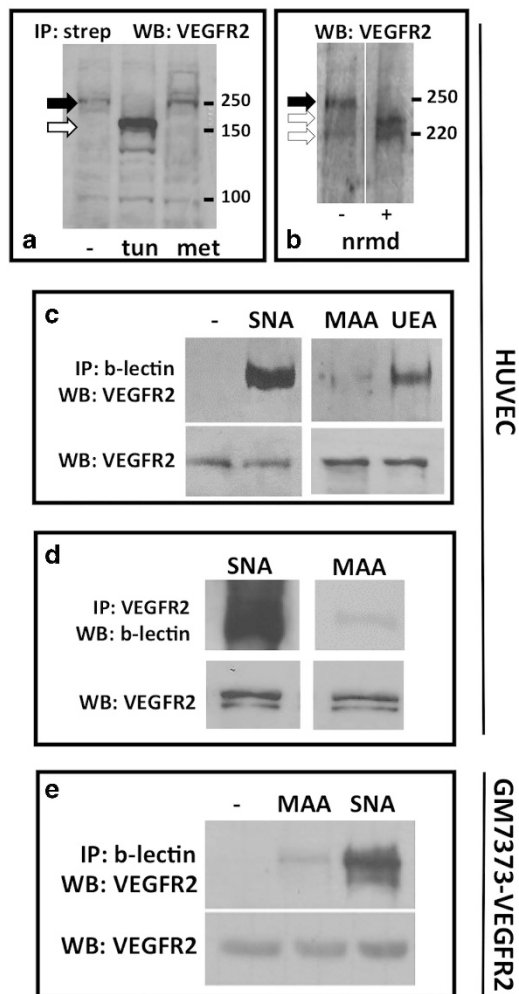


Figure 2. Glycosylation of VEGFR2 at the EC surface. (a) Proteins associated to the surface of HUVECs left untreated (-) or treated with tunicamycin (tun) or with vehicle methanol (met) were biotinylated, immunoprecipitated with streptavidin and analyzed by WB with anti-VEGFR2 antibody. (b) HUVECs were left untreated or treated with neuraminidase (nrmd), lysed, and analyzed by WB with anti-VEGFR2 antibody. In both the panels, black arrows point to the high molecular band corresponding to fully glycosylated VEGFR2. White arrows point instead to the low molecular weight bands corresponding to the de-glycosylated (a) or de-sialylated (b) forms of the receptor. HUVECs (c) or GM7373-VEGFR2 cells (e) were immunoprecipitated with the indicated biotinylated lectins (b-lectins) and analyzed by WB with anti-VEGFR2 antibody. Alternatively, HUVECs were immunoprecipitated with anti-VEGFR2 antibody and analyzed by WB with the indicated b-lectins (d). The experiments shown are representative of other 2–3 that gave similar results.

Next, the specific presence of NeuAc on VEGFR2 was investigated by neuraminidase digestion of the HUVEC surface. As shown in Figure 2b, incubation with neuraminidase causes a partial but significant decrease of the apparent MW of EC surface VEGFR2, thus indicating the presence of NeuAc residues on the receptor.

In a further series of experiments, sugar-binding lectins and immunoprecipitation experiments were used to characterize the linking of NeuAc to different positions on VEGFR2 glycans. In agreement with SPR analysis, both UEA-1 and SNA bind to endothelial VEGFR2 while the binding of MAA is negligible (Figure 2c). The selective binding of SNA, but not of MAA, to endothelial VEGFR2 was confirmed when the receptor was

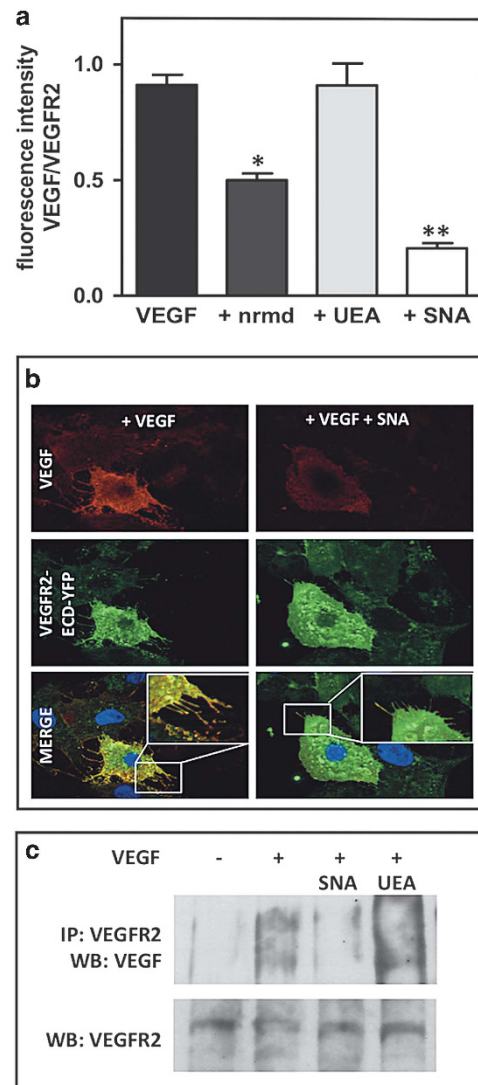


Figure 3. NeuAc and VEGF/VEGFR2 interaction at the EC surface. (a) Chlorate-treated fluorescent ECD-VEGFR2-EYFP GM7373 were incubated with neuraminidase (nrmd), with VEGF and the indicated lectins and analyzed in immunofluorescence with anti-VEGF antibody. Fluorescence intensity was expressed as described in material and methods. Data represent the media of 15–30 measurements for each sample. (* $P < 0.01$ and ** $P < 0.001$, respectively in respect to cell treated with VEGF alone). (b) Representative microphotographs of chlorate-treated ECD-VEGFR2-EYFP GM7373 cells incubated with VEGF and SNA. (c) HUVECs were incubated with VEGF and the indicated lectins, subjected to cross-linking, immunoprecipitated with anti-VEGFR2 antibody and analyzed by WB with anti-VEGF antibody (upper bands). Uniform loading was confirmed by WB with anti-VEGFR2 antibody of total lysates (lower bands). The experiment shown is representative of another one that gave similar results.

immunoprecipitated with anti-VEGFR2 antibody and analyzed by Western blot (WB) with biotinylated lectins (Figure 2d). To evaluate the presence of NeuAc also on VEGFR2 expressed at the surface of ECs different from HUVECs, the experiments were repeated on bovine ECs overexpressing human VEGFR2 (GM7373-VEGFR2 cells),³⁰ obtaining basically the same results (Figure 2e).

Taken together, all these results demonstrate that VEGFR2 expressed by different cell types contains glycans bearing fucose and $\alpha(2,6)$ -NeuAc, but not $\alpha(2,3)$ -NeuAc.

NeuAc and VEGF/VEGFR2 interaction at the EC surface

To assess whether VEGFR2-linked NeuAc contributes to the interaction of the receptor with VEGF, we used ECD-VEGFR2-EYFP GM7373 cells that overexpress VEGFR2 extracellular portion fused to the enhanced yellow fluorescent protein (EYFP).³¹ Before each experiment, these cells were treated with chlorate to remove HSPGs, whose binding to VEGF could mask the specific interaction of the growth factor with VEGFR2. Under these experimental conditions, VEGF colocalizes with EYFP-labeled VEGFR2 at the surface of ECD-VEGFR2-EYFP GM7373 cells. This association is prevented by pretreatment of ECs with neuraminidase or by incubation with SNA, but not with UEA-1 (Figures 3a and b), indicating that $\alpha(2,6)$ -linked NeuAc, but not fucose, mediates VEGF/VEGFR2 interaction. This was confirmed by the capacity of SNA, but not of UEA-1, to prevent VEGF/VEGFR2 interaction in cell-surface cross-linking experiments performed on HUVECs incubated with VEGF and lectins (Figure 3c). Thus, SNA retains its capacity to binds VEGFR2 also at the cell surface in the presence of VEGF, a condition in which receptor homodimerization and/or its coupling with coreceptors are favored.

NeuAc and VEGF/VEGFR2-mediated pro-angiogenic activation of ECs

As mentioned above, VEGF engagement causes VEGFR2 homodimerization and autophosphorylation.³ To better investigate the involvement of NeuAc in this process, VEGFR2 phosphorylation was evaluated in neuraminidase-treated or control ECs stimulated with VEGF in the absence or presence of SNA: the removal of surface-associated NeuAc by neuraminidase or its masking by SNA reduces the capacity of VEGF to induce VEGFR2 phosphorylation in HUVECs and GM7373-VEGFR2 cells, whereas UEA-1 is ineffective (Figure 4a). In a second set of experiments, to fully validate the specificity of the inhibitory effect of SNA on VEGFR2 phosphorylation, other lectins were taken in consideration. As shown in Supplementary Figure 1, PHA-L, GSL-IB₄ and MAA do not inhibit VEGF-dependent phosphorylation of VEGFR2. Importantly, with the exception of UEA-1, all the lectin tested are endowed with a MW that is similar to that of SNA (Table 1), ruling out the possibility that their different inhibitory capacity depends on their different size.

Beside VEGFR2, VEGF binds and activates also VEGFR1.⁷ Thus, a possible involvement of NeuAc in VEGF-dependent activation of VEGFR1 was evaluated. As shown in Figure 4b, the removal of surface-associated NeuAc by neuraminidase reduces also the capacity of VEGF to induce VEGFR1 phosphorylation in HUVECs.

As already mentioned, different isoforms of VEGF-A exist, including the two 121 and 165 amino acid isoforms (VEGF₁₂₁ and VEGF₁₆₅) that differ for the presence of the cationic heparin-binding domain involved in the interaction of VEGF₁₆₅ with polyanionic HSPGs. Due to the anionic nature of NeuAc, we decided to investigate whether the heparin-binding domain of VEGF₁₆₅ was involved in its binding to VEGFR2-associated NeuAc. As shown in Figure 4c, SNA inhibits VEGFR2 autophosphorylation mediated by VEGF₁₆₅ but not by VEGF₁₂₁, suggesting that the lectin specifically interferes with the interaction of VEGF₁₆₅ heparin-binding domain with NeuAc residues of VEGFR2 rather than by changing the stability of ligand-receptor complex.

Following VEGFR2 activation by VEGF, ECs acquire a pro-angiogenic phenotype characterized by increased cell motility and proliferation. Thus, the involvement of NeuAc in VEGF-dependent EC motility was evaluated in control and neuraminidase-treated HUVECs: VEGF induces an increase of HUVEC motility that is significantly reduced by neuraminidase treatment (Figure 4d). No effect was instead exerted by neuraminidase on basal cell motility, indicating that the enzymatic treatment does not cause a general impairment of the cell machinery. Accordingly, SNA inhibits HUVEC motility in response to VEGF whereas UEA-1 was

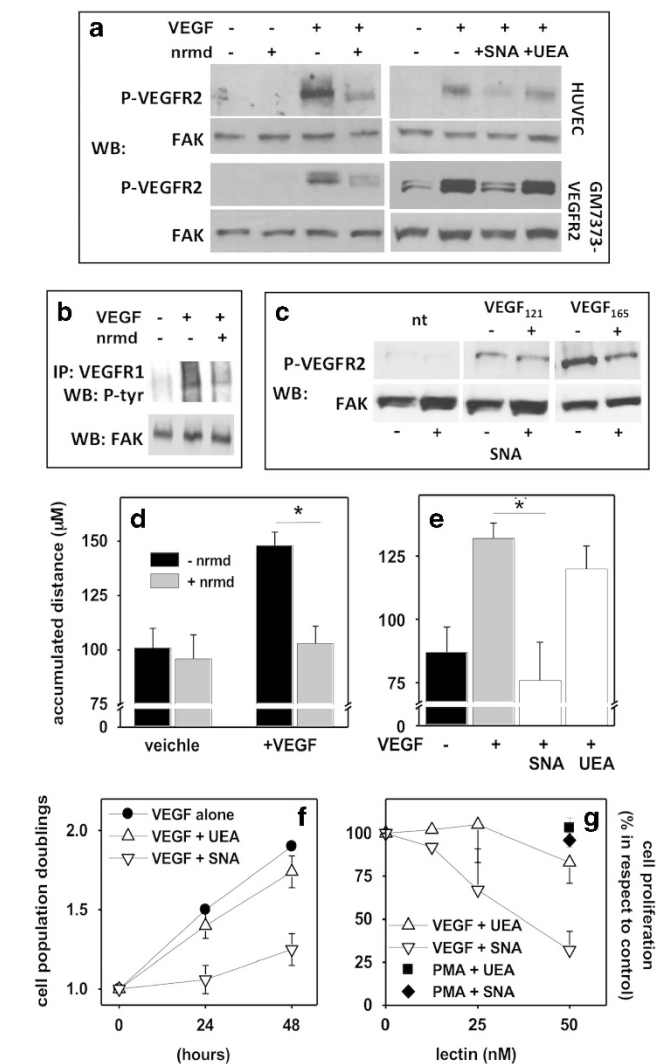


Figure 4. NeuAc and VEGF/VEGFR2-dependent pro-angiogenic activation of ECs *in vitro*. **(a, b)** ECs were treated with neuraminidase (nrmd) and stimulated with VEGF in the absence or in the presence of lectins. **(c)** ECs were stimulated with or without VEGF₁₆₅ or VEGF₁₂₁ in the presence of SNA. At the end of incubations, cells were lysed and analyzed by WB with anti-P-VEGFR2 antibody **(a, c)**, or immunoprecipitated with anti-VEGFR1 antibody and analyzed by WB with anti-phospho-tyrosine antibody (P-tyr) **(b)**. Uniform loading was confirmed by WB with anti-FAK antibody. The experiments shown are representative of two other that gave similar results. HUVECs were treated with VEGF after neuraminidase (nrmd) treatment **(d)** or in the presence of lectins **(e)** and assessed for motility (**P* < 0,01). The experiments shown are representative of two other that gave similar results. Alternatively, HUVECs were stimulated with VEGF or PMA and lectins (50 nM) for 24 or 48 h **(f)** or with increasing concentrations of lectins for 48 h **(g)**. Then, cells were counted. Each value is the mean \pm s.e.m. of three independent experiments.

ineffective (Figure 4e). In addition, SNA does not inhibit EC motility induced by the PKC-activating phorbol-12-myristate-13-acetate (PMA)³² further supporting the specificity of the effect (data not shown).

We then investigated the role of NeuAc on VEGF-dependent EC proliferation: HUVECs undergo 1.5 and 1.8 cell population doublings at 24 h and 48 h after stimulation with VEGF, respectively (Figure 4f). SNA inhibits VEGF-dependent HUVEC proliferation in a time- and dose-dependent manner (Figures 4f and g). The inhibition is specific since UEA-1 is ineffective

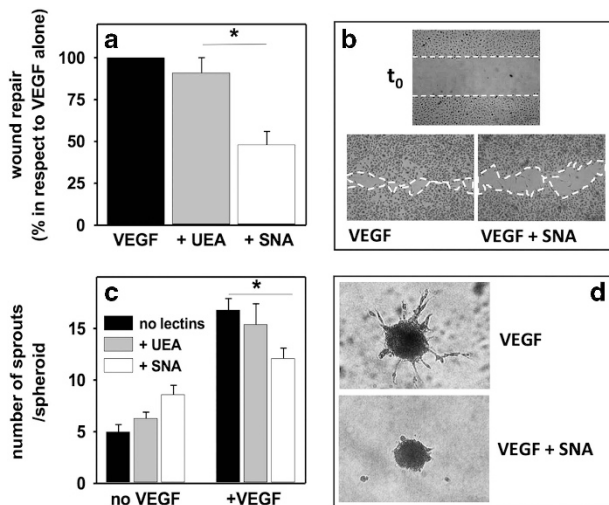


Figure 5. Effect of lectins on VEGF-dependent EC motogenesis and sprouting. **(a)** HUVEC monolayers were wounded and incubated with VEGF and lectins. Then, the extension of the repaired wound area was evaluated ($*P < 0.05$). **(b)** Representative microphotographs of wounded HUVEC monolayers taken at the start of experiment (t_0) and after 24 h of incubation with VEGF and SNA. Dashed lines mark the edge of the wound at t_0 . White areas mark the wound extension after 24 h. **(c)** HUVEC spheroids embedded in fibrin gel were incubated with VEGF and lectins. Then, radially growing cell sprouts were counted. ($*P < 0.05$). **(d)** Representative microphotographs of spheroids incubated with VEGF and SNA. Each value is the mean \pm s.e.m. of three independent experiments.

Time (h)	untreated	+ SNA	+ UEA-1	+ neuraminidase
6	100	104 \pm 6	109 \pm 5	89 \pm 9
24	100	98 \pm 8	107 \pm 6	Not performed
48	100	101 \pm 7	115 \pm 8	Not performed

HUVECs were incubated at 37 °C for the indicated periods of time in the absence (untreated) or in the presence of the indicated lectins (50 nM) or after treatment with neuraminidase (125 mU/ml). Then cells were subjected to MTT assay. Data are expressed as percentage of surviving cells after the various treatment in respect to untreated cells.

(Figures 4f and g) and both lectins do not affect PMA-induced proliferation (Figure 4g) nor HUVEC vitality (Table 2). At variance with EC motility, VEGF-dependent proliferation is unaffected when measured at 24 and 48 h after neuraminidase treatment (data not shown), likely due to the rapid recovery of VEGFR2 sialylation at the EC surface that occurs within 4–6 h after enzymatic digestion (Supplementary Figure 2A).

The ability of VEGF to induce proliferation and motility results in an increased regenerative potential that allows the repair of a mechanically wounded EC monolayer (motogenic activity).³³ As shown in Figures 5a and b, SNA inhibits VEGF motogenic activity in wounded HUVEC monolayers whereas UEA-1 is ineffective.

Finally, the effect of lectins was evaluated in an *in vitro* tridimensional model of angiogenesis in which EC spheroids stimulated by angiogenic growth factors invade a three-dimensional fibrin matrix, generating endothelial sprouts as a result of the localized breakdown of the extracellular matrix that occurs together with EC migration and growth.³⁴ As shown in Figure 5c, VEGF increases the number of sprouts that originate from EC spheroids. SNA, but not UEA-1, causes a reduction of VEGF-dependent HUVEC sprouting (Figures 5c and d).

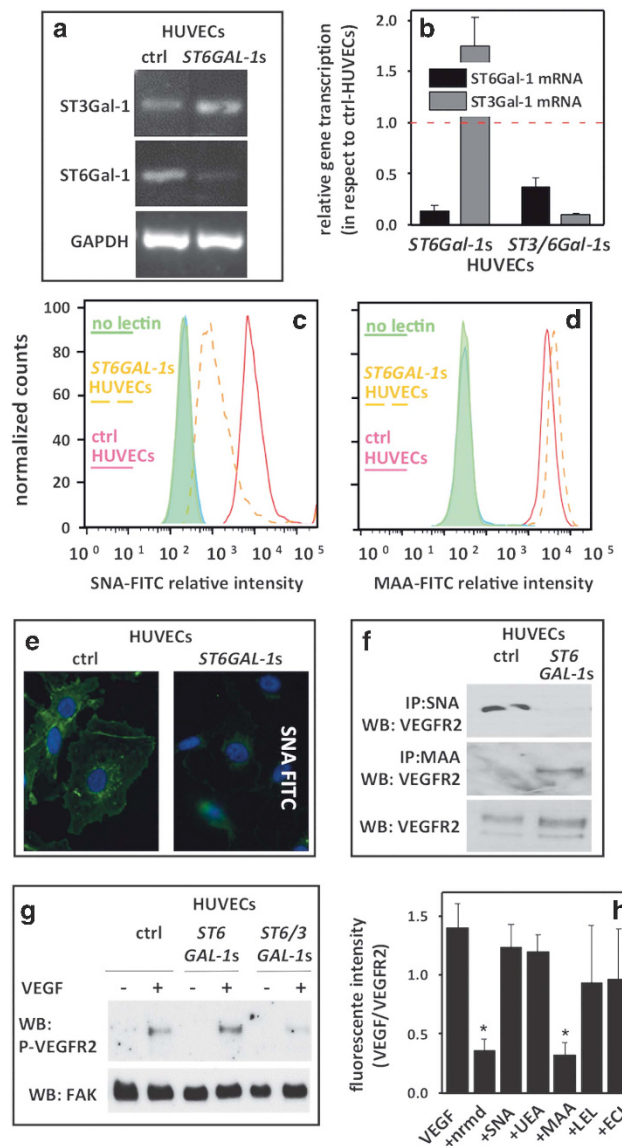


Figure 6. Effect of STs knockdown on VEGFR2 glycosylation, VEGF binding and VEGFR2 autophosphorylation. **(a)** RT-PCR analysis of ST6Gal-1 and ST3Gal-1 mRNA levels in HUVECs. GAPDH: 23, ST6Gal-1 and ST3Gal-1: 28 amplification cycles. **(b)** Quantitative RT-PCR analysis of ST6Gal-1 and ST3Gal-1 mRNA levels in *ST6GAL-1s-* and *ST3/6GAL-1s-*HUVECs. Data are expressed as fold change of target gene transcription in respect to ctrl-HUVECs (red dashed line), normalized to the internal standard control gene (GAPDH). **(c, d)** Ctrl- or *ST6GAL-1s-*HUVECs were stained with SNA-FITC or MAA-FITC and analyzed by flow cytometry. **(e)** Representative microphotographs of ctrl- or *ST6GAL-1s-*HUVECs decorated with SNA-FITC and analyzed by immunofluorescence using a Zeiss Axiovert 200M epifluorescence microscope. **(f)** Ctrl- and *ST6GAL-1s-*HUVECs were immunoprecipitated with the indicated biotinylated lectins and analyzed by WB with anti-VEGFR2 antibody. **(g)** Ctrl-, *ST6GAL-1s-* and *ST3/6GAL-1s-*HUVECs were stimulated with or without VEGF and analyzed by WB with anti-P-VEGFR2 antibody. Uniform loading was confirmed by WB with anti-FAK antibody. The experiments shown are representative of another one (**a, c–f**) or two (**b, g**) that gave similar results. **(h)** Quantification of the fluorescence intensity (expressed as VEGF/VEGFR2 ratio) of fluorescent ECD-VEGFR2-EYFP-A745 CHO-K1 treated with or without neuraminidase (nrmd) and incubated with VEGF and the indicated lectins and analyzed in immunofluorescence with anti-VEGF antibody. Data represents the media of 10–20 measurements for each sample. ($*P < 0.001$).

In conclusion, various *in vitro* observations demonstrate that $\alpha(2,6)$ -linked NeuAc mediates VEGF/VEGFR2 interaction and consequent activation of a pro-angiogenic phenotype in ECs.

Sialyltransferase knockdown, VEGFR2 glycosylation and biological activity

ST6Gal-1 and ST3Gal-1 catalyze the addition of NeuAc to galactose residues of glycoprotein polysaccharide chains *via* $\alpha(2,6)$ and $\alpha(2,3)$ glycosidic bonds, respectively.³⁵

To investigate the role of $\alpha(2,6)$ -NeuAc in VEGFR2 activation, the *ST6GAL-1* gene was silenced in HUVECs using a lentiviral vector harboring an appropriate short hairpin RNA (shRNA). As shown in Figure 6a, semi-quantitative reverse transcription PCR (RT-PCR) analysis indicates that HUVECs express *ST6GAL-1* and *ST3GAL-1* at similar levels. *ST6GAL-1* knockdown in *ST6GAL-1* silenced HUVECs (*ST6GAL-1s*-HUVECs) causes a dramatic decrease of the steady-state levels of the corresponding transcript in parallel with an increase of *ST3GAL-1* transcription. These results were confirmed by quantitative RT-PCR (qRT-PCR) analysis, where the increase of *ST3GAL-1* transcription was even more evident (Figure 6b). Taken together, these results suggest that a 'compensation' links the decrease of *ST6Gal-1* mRNA to the increase of *ST3Gal-1* mRNA. In agreement with these transcriptional changes, *ST6GAL-1* silencing inhibits the binding of SNA to the surface of *ST6GAL-1s*-HUVECs (Figures 6c–e) and to endothelial VEGFR2 in particular (Figure 6f). Again in keeping with the increase of *ST3GAL-1* transcription, *ST6GAL-1* silencing causes an increase of the interaction of MAA with the surface of *ST6GAL-1s*-HUVECs and with VEGFR2 in particular (Figures 6d and f). These data prompted us to evaluate if the increase of $\alpha(2,3)$ -linked NeuAc represents a compensatory mechanism to overcome the reduction of $\alpha(2,6)$ -linked NeuAc. Indeed, VEGF retains its capacity to induce VEGFR2 activation in *ST6GAL-1s*-HUVECs at levels comparable to control cells (Figure 6g), suggesting that $\alpha(2,3)$ -linked NeuAc can functionally replace $\alpha(2,6)$ -linked NeuAc.

To confirm this possibility, we studied VEGF binding to VEGFR2 in A745 CHO-K1 cells that spontaneously lack the *ST6Gal-1* enzyme,³⁶ express low levels of HSPGs³⁷ and that were stably transfected to overexpress an EYFP-tagged VEGFR2 (ECD-VEGFR2-EYFP-A745 CHO-K1 cells). In these cells, VEGF/VEGFR2 interaction occurs also in the absence of $\alpha(2,6)$ -linked NeuAc and is inhibited by neuraminidase treatment and, due to the specific $\alpha(2,3)$ sialylation of these cells, by MAA. The specificity of this latter inhibitory effect is proven by the observation that, in the same experimental conditions, lectins SNA, UEA-1, LEL or ECL are ineffective (Figure 6h). Together, these data confirm that $\alpha(2,3)$ -linked NeuAc can functionally replace $\alpha(2,6)$ -linked NeuAc on VEGFR2.

In a final effort, we sought to evaluate if the functional *ST3Gal-1*-dependent compensation observed after *ST6GAL-1* silencing could be abolished by neutralizing the two STs at once. To this purpose, a double knockout was performed to silence both the *ST6GAL-1* and *ST3GAL-1* genes simultaneously, generating the *ST3/6GAL-1s*-HUVECs. qRT-PCR analysis revealed that the double silencing effectively inhibits the transcription of both the targeted STs (Figure 6b). At a functional level, the simultaneous silencing of *ST6GAL-1* and *ST3GAL-1* genes prevents VEGF-dependent autophosphorylation of VEGFR2 in *ST3/6GAL-1s*-HUVECs (Figure 6g), further sustaining the role of VEGFR2 sialylation in mediating the pro-angiogenic activity of VEGF.

SNA and VEGF/VEGFR2-dependent angiogenesis

Our observations rise the hypothesis that NeuAc-binding lectin(s) may represent a novel tool to suppress VEGF/VEGFR2-dependent neovascularization. To confirm this possibility, the VEGF-inhibitory activity of SNA was assessed in different *ex vivo* and *in vivo* models of angiogenesis. To this aim, SNA was evaluated in a murine retina

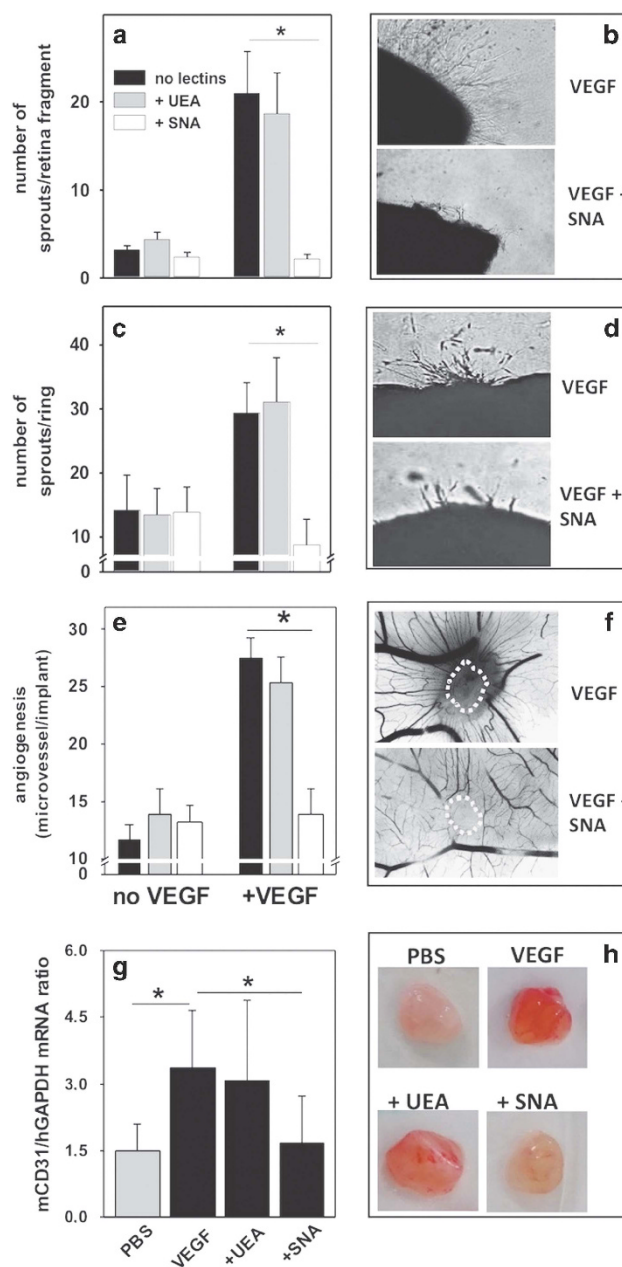


Figure 7. Effect of lectins in *ex vivo* and *in vivo* models of VEGF/VEGFR2-dependent angiogenesis. Fragments of murine retina (a) or human artery ring (c) embedded in fibrin gel were incubated with VEGF and lectins. Then, radially growing cell sprouts were counted. (**P* < 0.05). Representative microphotographs of murine retina fragments (b) or human artery ring (d) incubated with VEGF and SNA. (e) CAMs were implanted with alginate beads adsorbed with VEGF and lectins. Then the angiogenic response was scored. (f) Representative photographs of CAMs incubated with VEGF and SNA. Each value is the mean \pm s.e.m. of two (a, e) or three (c) independent experiments. (g) C57BL/6 mice were injected subcutaneously with Matrigel containing FGF2 and VEGF in the absence or the presence of the indicated lectins. One week later plugs were harvested and processed for qRT-PCR. The mRNA expression levels of murine CD31 were normalized to the levels of human GAPDH and expressed as murine CD31/human GAPDH mRNA ratio. (**P* < 0.05). (h) Representative photographs of Matrigel plugs in the indicated experimental conditions.

angiogenesis (EMRA) assay, an *ex vivo* model that allows the maintenance of the integrity of the retinal structure and represents a valid method to assess the response of sprouting ECs to chemical modulation.³⁸ As shown in Figures 7a and b, VEGF induces an increase of the number of EC sprouts that originate from retina fragments and this activity is fully inhibited by SNA but not by UEA-1. Similar results were obtained when the two lectins were tested for the capacity to affect the VEGF-induced sprouting of ECs in a human umbilical artery ring aorta assay³⁰ (Figures 7c and d).

Finally, the effect of SNA was evaluated *in vivo*. In a first series of experiments, the chick-embryo chorioallantoic membrane (CAM) assay³⁹ was exploited. As shown in Figures 7e and f, VEGF induces a potent neovascular response in the CAM that is fully inhibited by SNA whereas UEA-1 is again ineffective. Notably, SNA does not affect the spontaneous developmental neovascularization that occurs in the CAM in the absence of VEGF, thus confirming the specificity of the effect. Then, to further support the possibility that NeuAc blockage by lectins possesses a therapeutic value in inhibiting VEGF/VEGFR2-mediated neovascularization, Matrigel plug assay in mice was performed. As shown in Figure 7g, a mixture of VEGF and FGF2 induces a significant neovascularization in mice injected subcutaneously with Matrigel and this angiogenic response is significantly inhibited by SNA but not by UEA-1.

DISCUSSION

VEGF represents the most important angiogenic growth factor able to activate EC surface VEGFR2.³ Even though the structural determinants of VEGFR2 protein required to bind VEGF have been deeply investigated,^{40–42} the contribution of VEGFR2 glycosylation to VEGF engagement remains to be fully elucidated. Indeed, although VEGFR2 activity has been proposed to be glycosylation-independent,¹⁴ experimental evidences indicate that an appropriate glycosylation is crucial for VEGFR2 stability, intracellular delivery, surface expression^{9,10} and pro-angiogenic activity.^{10,13} A first effort at profiling VEGFR2 glycosylation has been made by Chandler *et al.*⁴³ that, by means of mass spectrometry, demonstrated the presence of NeuAc on *N*-glycans of VEGFR2. However, since NeuAc residues have been found also on the receptor *O*-glycans,⁴⁴ further studies are required to fully characterize its sialylation.

We found that tunicamycin, by inhibiting VEGFR2 glycosylation, causes the accumulation at the cell surface of a low molecular weight VEGFR2 that is unable to undergo VEGF-dependent autophosphorylation in ECs (P Chioldelli, unpublished observations). On these bases, the role of VEGFR2 glycosylation in angiogenesis was here investigated by a comprehensive approach based on pharmacologic, enzymatic and genetic methods.

The use of the specific sugar-binding lectins SNA and MAA, that bind NeuAc linked to different glycan positions, demonstrated that NeuAc is present on VEGFR2-associated glycans in position $\alpha(2,6)$, but not in position $\alpha(2,3)$, when ECs are grown under standard conditions. Masking of $\alpha(2,6)$ -linked NeuAc by SNA inhibits VEGF/VEGFR2 interaction and VEGFR2 autophosphorylation. At variance, fucose-binding UEA-1 interacts with VEGFR2 without hampering VEGF/VEGFR2 interaction nor VEGFR2 autophosphorylation. Together, these observations point to a role for VEGFR2-associated NeuAc, but not VEGFR2-associated fucose, in VEGFR2-driven angiogenic responses. Accordingly, SNA inhibits VEGF angiogenic activity *in vivo* and in wide range of *in vitro* and *ex vivo* assays representative of the whole pro-angiogenic EC activation process, whereas UEA-1, as well as other lectins, is ineffective. Thus, the inhibitory activity of SNA does not appear to be due to a change in the stability of the VEGF/VEGFR2 interaction or to an aspecific steric hindrance, but more likely, it depends on a specific masking of $\alpha(2,6)$ -linked NeuAc required to the receptor to bind to the cationic heparin-binding domain

present in VEGF. This is further supported by the observations that the second and third Ig-homology domains of VEGFR2 involved in VEGF interaction⁴² bear Asn residues that are attachment sites for *N*-linked glycans⁴⁵ and that SNA inhibits VEGFR2 phosphorylation induced by VEGF₁₆₅ but not that by VEGF₁₂₁ (that is devoid of the heparin-binding domain).

In keeping with these observations, treatment of ECs with neuraminidase effectively removes VEGFR2-associated NeuAc and inhibits VEGF/VEGFR2 interaction and receptor autophosphorylation. This resulted in the inability of neuraminidase-treated cells to respond to VEGF stimulation in a short-term migration assay. Neuraminidase-induced VEGFR2 de-sialylation is transient, the reappearance of the fully sialylated receptor occurring 4–6 h after enzymatic treatment (Supplementary Figure 2A). BFA, an inhibitor of the endoplasmic reticulum-Golgi apparatus passage, inhibits VEGFR2 re-sialylation causing the accumulation of a low molecular weight (possibly non-sialylated) form of the receptor in the cell (Supplementary Figure 2B). Relevant to this point, STs are found in the Golgi apparatus, in post-Golgi vesicles and even on the plasma membrane in different cell types,^{46,47} suggesting that also in ECs the rapid re-sialylation of VEGFR2 may undergo in these same structures.

The quick process of VEGFR2 sialylation differs from what observed for integrin $\alpha_v\beta_3$, whose sialylated form slowly reappears on EC surface 48 h after neuraminidase treatment.²⁰ Apparently, the endothelium can stand a prolonged de-sialylation of $\alpha_v\beta_3$ (whose function might be surrogated by other integrins), but not of VEGFR2, pointing to a pivotal role of NeuAc in VEGFR2 biology.

The requirement of VEGFR2-associated NeuAc for its binding to VEGF and for consequent biological activities have been here demonstrated both in a 'cell-free' model (SPR analysis) by means of the highly purified, surface-immobilized receptor and directly at the surface of the cell (a more physiological environment where VEGFR2 homodimerizes and couples with its coreceptors in the presence of VEGF). Given the dramatic changes in glycosylation pattern of individual cell types,²⁹ it is also important to note that the role of NeuAc in VEGF/VEGFR2 interaction has been confirmed in different cell types (human or bovine ECs, hamster epithelial cells).

The expression of glycosyltransferases is modulated in activated ECs^{48,49} and the overexpression of the sialyltransferase ST6Gal-1 dose-dependently counteracts neuraminidase-mediated inhibition of EC tube formation *in vitro*.⁵⁰ Here we demonstrate that, despite HUVECs express both ST6Gal-1 and ST3Gal-1 in standard culture conditions, VEGFR2 sialylation remains restricted to $\alpha(2,6)$ glycosidic bonds, ensuring VEGF-dependent receptor activation and consequent EC pro-angiogenic activation. It remains possible however that, during the dramatic modifications of glycosylation that occur during EC activation,^{18,51} different STs modulate the specific sialylation(s) of other receptors, driving the binding of different angiogenic growth factors. In effect, ST6Gal-1 overexpression in ECs increases $\alpha(2,6)$ -linked NeuAc on different proteins but not on VCAM-1⁴⁹ and the absence of $\alpha(2,6)$ -linked NeuAc on the EC surface enhances the binding of VEGFR2 to galectin-1, activating an alternative pro-angiogenic signaling.¹⁴

Notably, the silencing of *ST6GAL-1* gene leads to an effective reduction of related mRNA and of VEGFR2-linked $\alpha(2,6)$ -NeuAc in HUVECs, paralleled by a concomitant increase of *ST3GAL-1* mRNA and of $\alpha(2,3)$ -sialylation of the receptor. Further studies are required to ascertain if, beside the transcriptional regulation of *ST6GAL-1* and *ST3GAL-1* genes here demonstrated, other epigenetic mechanisms contribute to the control of VEGFR2 sialylation (that is, *ST6Gal-1* protein degradation, further discussed in the next paragraph). Whatever the mechanism, *ST6Gal-1* inactivation generates an alternative 'sialylation profile' of VEGFR2 that remains biologically functional, as demonstrated by the observation that $\alpha(2,3)$ -sialylated VEGFR2 retains its capacity to bind VEGF and to undergo VEGF-dependent autophosphorylation at the

surface of genetically ST6Gal-1-deficient CHO-K1 cells (Figures 6g and h). Accordingly, preliminary experiments indicate that the shift from $\alpha(2,6)$ -NeuAc to $\alpha(2,3)$ -NeuAc does not modify the affinity of the VEGF/VEGFR2 interaction (P Chiodelli, unpublished observations).

The 'alternative' $\alpha(2,3)$ sialylation of VEGFR2 may be required in all those settings in which $\alpha(2,6)$ sialylation of VEGFR2 is hampered, such as during an abnormal EC stimulation by TNF- α , that leads to the proteolytic degradation of ST6Gal-1.⁵² ST6Gal-1 may be cleaved also by β -secretase (BACE1), an hypoxia-inducible pro-angiogenic factor expressed by EC.^{53,54} Finally, *ST6GAL-1* gene transcription may be inhibited by specific DNA methylation of its promoter region.⁵⁵ Thus, VEGFR2 can counteract a selective impairment of its sialylation profile by shifting the linking of NeuAc to other positions as to maintain a sialylation state that ensures the functionality of VEGFR2 in EC homeostasis and pro-angiogenic activation. These observations further sustain the hypothesis of an important role of VEGFR2-associated NeuAc in VEGF-dependent angiogenesis.

Our observations point to NeuAc-binding lectins as a starting point for the development of antiangiogenic compounds targeting VEGFR2 glycosylation. Even though NeuAc is extensively present on the EC surface, experimental evidences suggest the possibility of tailoring NeuAc-targeted approaches. (i) At variance with VEGF, galectin-1 binds VEGFR2 and induces EC activation only in the absence of $\alpha(2,6)$ -NeuAc.¹⁴ (ii) EC incubation with neuraminidase does not affect VEGFR2 autophosphorylation triggered by HIV-1 Tat but prevents its interaction with desialylated $\alpha_v\beta_3$ integrin, thus inhibiting its angiogenic activity.²⁰ (iii) Similarly, HIV-1 Tat/ $\alpha_v\beta_3$ interaction and angiogenic activity can be inhibited by MAA.²⁰ (iv) Both SNA and MAA modulate fibroblast growth factor 2 (FGF2) interaction with $\alpha_v\beta_3$ but not with the heavily sialylated FGF receptor 1 (P Chiodelli, manuscript in preparation).

In order to induce a full angiogenic response in ECs, VEGFs need to interact also with other members of the VEGFR family and with coreceptors. Regarding the formers, here we demonstrated that NeuAc is necessary also for VEGF-dependent activation of VEGFR1. Regarding VEGF coreceptors instead, $\alpha_v\beta_3$ integrin⁵ and neuropilin-1⁶ are heavily sialylated,^{20,56} suggesting that masking NeuAc of EC surface receptors other than VEGFR2 may contribute to the antiangiogenic effects of SNA. However, it is undeniable that, in our experimental conditions, SNA exerts its antiangiogenic effect mainly by a direct interaction with VEGFR2, as demonstrated by specific SPR and immunoprecipitation experiments (Figures 1 and 2).

The possible involvement of NeuAc in the pro-angiogenic activity of other receptors/angiogenic growth factors points to this sugar as a hub/docking structure whose appropriate inhibition may disable various pro-angiogenic signaling networks, thus exerting possible multiple-targeting effects. In this frame, NeuAc-binding lectins may represent the basis for the development of antiangiogenic compounds with therapeutic implications in angiogenesis-dependent diseases, including cancer.

MATERIALS AND METHODS

Reagents

VEGF-A₁₆₅ and VEGF₁₂₁ were provided by K. Ballmer-Hofer (PSI, Villigen, Switzerland). FGF2 was from Tecnogen (Piana di Montevarna, Caserta, Italy). Lectins from *Maackia amurensis* (MAA), *Sambucus nigra* (SNA), *Ulex europaeus* (UEA-1), *Phaseolus vulgaris* (L-PHA), *Lycopersicon esculentum* (LEL), *Erythrina cristagalli* (ECL), *Griffonia simplicifolia* (GSL-IB₄) and their biotinylated forms were from Vector Laboratories (Burlingame, CA, USA). Biotinylated UEA-1 was from EY laboratories (San Mateo, CA, USA). For the molecular weight (MW) and specific sugar residues recognized by these lectins, see Table 1. Phorbol-12-myristate-13-acetate, tunicamycin, brefeldin-A (BFA) and neuraminidase from *Clostridium perfringens* were

from Sigma (St Louis, MO, USA). The monomeric recombinant form of VEGFR2 fused to Fc produced in murine myeloma cells from ImmunoSource (Zoersel, Belgium). Human Ig Fc fragment and antibody against phospho-tyrosine (clone 4G10) from Millipore (Bedford, MA, USA). Monoclonal Y1175 antibody directed against phosphorylated VEGFR2 (MA5-15170) from Thermo Scientific (Waltham, MA, USA). Antibodies directed against focal adhesion kinase (FAK, sc-558), unphosphorylated VEGFR2 (sc-504) and VEGFR1 (sc-316) and horseradish peroxidase (HRP)-labeled anti-rabbit antibody from Santa Cruz Biotechnology (Santa Cruz, CA, USA). Antibody directed against VEGF-A₁₆₅ (MAB293) from R&D System (Minneapolis, MN, USA). Alexa Fluor 594 anti-mouse IgG from Thermo Scientific. Sodium chlorate from BDH Laboratory Supplies (Pole, United Kingdom). Matrigel (Cultrex BME Growth Factor Reduced) from Trevigen (Gaithersburg, MD, USA).

SPR assay

SPR measurements were performed on a BIAcore X100 instrument and research-grade CM5 sensorchips (GE-Healthcare, Milwaukee, WI, USA). VEGFR2-Fc or the Fc fragment (used as a negative control for blank subtraction) (20 μ g/ml in 10 mM sodium acetate pH 4.0) were allowed to react with two separate flow cells of a CM5 sensorchip pre-activated as described,²⁰ leading to the immobilization of 11 760 and 4424 RU (approximately 80 fmol/mm² for both the proteins). Increasing concentrations of VEGF or of the different lectins in HBS-EP buffer (GE-Healthcare) were injected over the VEGFR2 or Fc surfaces for 120 s and then washed until dissociation (600 s). Binding parameters were calculated as described.⁵⁷

Cell cultures

Human umbilical vein ECs (HUVECs) at passages I-VI were grown on plastic surface coated with porcine gelatine (Sigma) in M199 medium containing 20% fetal calf serum (FCS, Gibco Life Technologies, Grand Island, NY, USA), EC growth factor (100 μ g/ml) and porcine heparin (Sigma) (100 μ g/ml). Fetal bovine aortic endothelial GM7373 (from the Human Genetic Mutant Cell Repository, Institute for Medical Research, Camden, NJ, USA) cells were transfected with a pcDNA3.1 expression vector harboring the mouse VEGFR2 cDNA (provided by G Breier, Max Planck Institute, Bad Nauheim, Germany) to generate stable GM7373-VEGFR2 transfectant cells.³⁰ Alternatively, GM7373 cells were transfected with a pcDNA3/Enhanced Yellow Fluorescent Protein (EYFP) vector harboring the extracellular domain of human VEGFR2 (ECD-VEGFR2) cDNA (provided by K. Ballmer-Hofer, PSI, Villigen, Switzerland) to generate stable ECD-VEGFR2-EYFP GM7373 cells. Parental GM7373 cells and transfectants were grown in Dulbecco's modified Eagle medium (DMEM, Gibco Life Technologies) containing 10% FCS, vitamins, essential and non-essential amino acids. GAG-deficient A745 CHO-K1 cells³⁷ were kindly provided by JD Esko (University of California, La Jolla, CA, USA) and grown in Ham's F-12 medium containing 10% FCS. They were transfected with the ECD-VEGFR2 cDNA described above to generate stable ECD-VEGFR2-EYFP-A745 CHO-K1 cells. All cell lines were confirmed to be mycoplasma-free by standard 4,6-diamidino-2-phenylindole analysis.

shRNA-mediated silencing of β -galactoside sialyltransferases genes

pLKO.1 lentiviral vectors bearing *ST6GAL-1* or *ST3GAL-1* shRNA (targeting sequences: CGTGTGCTACTACTACCAG_TRCN0000035432 and GCTGGGAGA TAATGTCAGCAT_TRCN0000035551, Sigma) were used to knockdown the expression of the two STs in HUVECs. Briefly, cells maintained in complete medium were transduced by an 18 h incubation at 37 °C with non-targeting lentiviral vectors (ctrl-HUVECs), with the vector harboring the *ST6GAL-1* shRNA alone or with both the vectors harboring *ST6GAL-1* and *ST3GAL-1* shRNAs (*ST6GAL-1s*- and *ST3/6GAL-1s*-HUVECs, respectively). 48 h after infection, complete medium containing puromycin (0.5 μ g/ml) was used to select infected cells that were used for subsequent experiments until VI passage.

RT-PCR analysis

Total RNA was isolated from HUVECs by the TRIzol method. Aliquots (2 μ g/20 μ l) were retro-transcribed with MMLV reverse transcriptase (Invitrogen) using random hexaprimers. Then, 1/10th of the reaction was analyzed by RT-PCR for one cycle at 95 °C (5 min) and 23 cycles (GAPDH) or 27 cycles (others) at 94 °C, 67 °C, and 72 °C (1 min each). Aliquots (5 μ l) were

separated on a 1% agarose gel and visualized by Gel Red Nucleic Acid Stain (Biotium, Hayward, CA, USA). Alternatively, relative mRNA levels were quantified by real-time RT-PCR assays, using GAPDH as reference gene. Amplification and detection were performed with the ViiA7 Real-Time PCR Detection System (Applied Biosystem, Foster City, CA, USA); the fluorescence signal was generated by SYBR Green I. The following human primers were used:

hST3GAL1-FW:5'-GACTTGGAGTGGGTGGTGAG-3'
RV: 5'GGAACCGGGATGTAGGTGT-3';
hST6GAL1-FW:5'-CTCCCCAGAAGAGATTCAGC-3'
RV: 5'-TGGTCACACAGCGTCATCAT3'
hGAPDH-FW:5'-GAAGGTCGGAGTCAACGGATT-3',
RV:5'-TGACGGTGCCATGGAATTTG-3'.

Cell starvation, chlorate, tunicamycin, neuraminidase and BFA treatments

Cell starvation, was obtained by a 5 h incubation at 37 °C with M199 containing 5% FCS. To remove high capacity VEGF-binding sites associates to HSPGs, cells were incubated (48 h at 37 °C) with 50 mM chlorate to inhibit sulfation of HS chains. To prevent glycosylation of surface proteins, cells were incubated (24 h at 37 °C) with tunicamycin (2.0 µg/ml). To remove cell-surface-associated NeuAc cells were incubated (1 h at 37 °C) with neuraminidase (125 mU/ml). To inhibit exocytosis, cells were pre-treated for 3 h at 37 °C with BFA (1.0 µg/ml), subjected to neuraminidase treatment, added again with the same dose of BFA and incubated for the appropriate periods of time.

Biotinylation of EC surface proteins

HUVECs were incubated (2 h at 4 °C) with biotin-3-sulfo-*N*-hydroxy-succinimide ester sodium salt (Sigma) (0.5 mg/ml) in Hanks' Balanced Salt Solution. Cells were then lysed in 50 mM Tris-HCl buffer (pH 7.4) containing 150 mM NaCl, 1% Triton X-100, 1.0 mM Na₂VO₄, and protease inhibitors (lysis buffer). Samples (1.0 mg of protein) were immunoprecipitated with streptavidin-sepharose (GE-Healthcare), separated on SDS-7.5% PAGE and analyzed by WB with anti-VEGFR2 antibody.

FACS analysis

HUVECs were detached using M199 containing 5 mM EDTA at 37 °C and washed with PBS. Then cells were stained with SNA-FITC or MAA-FITC (Vector laboratories) for 20 min at 4 °C. Then, cells were washed with PBS and analyzed by MACSQuant cytofluorimeter (Miltenyi Biotec GmbH, Bergisch Gladbach, Germany). Data were analyzed with FlowJo software (Ashland, OR, USA).

VEGF/VEGFR2 binding assay

Chlorate-treated ECD-VEGFR2-EYFP GM7373 or ECD-VEGFR2-EYFP-A745 CHO-K1 cells were treated with neuraminidase and incubated (90 min at 4 °C) in Hanks' Balanced Salt Solution with calcium and magnesium containing VEGF (5.0 nM) and lectins (200 nM). Then, cells were washed with PBS and fixed in 4% paraformaldehyde. Immunofluorescence analysis was performed using an anti-VEGF antibody followed by Alexa Fluor 594 anti-mouse IgG (Invitrogen), and cells were photographed using a Zeiss Axiovert 200M epifluorescence microscope (Carl Zeiss, Gottingen, Germany). Fluorescence was quantified as corrected total cell fluorescence: integrated density—(area of selected cell × mean fluorescence of background).

VEGF/VEGFR2 cross-linking assay

This assay was performed as described³⁰ using HUVECs treated with VEGF at 5.0 nM and lectins at 200 nM. WB was performed with anti-VEGF antibody.

VEGFR phosphorylation assay

HUVECs or GM7373-VEGFR2 cells were starved, incubated (7 min at 37 °C) with VEGF₁₆₅ or VEGF₁₂₁ (0.5 nM) and lectins (50 nM) and lysed in lysis buffer. Then, for VEGFR2 analysis, 40 µg protein/sample were separated by SDS-7.5% PAGE followed and analyses by WB with antibody directed against the phosphorylated form of VEGFR2. At variance, for VEGFR1 analysis, 1 mg protein/samples from lysates of HUVECs treated with 2 nM of

VEGF₁₆₅ were immunoprecipitated with anti-VEGFR1 antibody and analyses by WB with antibody directed against total phospho-tyrosine.

Time-lapse videomicroscopy EC motility assay

This assay was performed as described³⁰ using VEGF at 0.5 nM and lectins at 50 nM.

Proliferation assay

HUVECs were seeded at 17 500 cells/cm² onto tissue culture multiwell plates in M199 containing 2.5% FCS. The following day cells were incubated (24 or 48 h at 37 °C) with VEGF (1.5 nM) or PMA (150 nM) and lectins. Then, cells were counted.

Wound monolayer assay

Confluent cultures of HUVECs were starved, wounded with a rubber policeman and incubated (24 h at 37 °C) with VEGF (1.5 nM) and lectins (100 nM). Then, the extent of wound repair was evaluated by measuring the area of the wound by computerized image analysis using the ImageJ software (<http://rsbweb.nih.gov/ij/>).

EC sprouting assay

This assay was performed as described⁵⁸ using VEGF at 1.5 nM and lectins at 100 nM.

MTT assay

HUVECs were treated with neuraminidase or lectins as described above and incubated in M199 containing 20% FCS. Then, MTT solution (3 mg/ml) was added. After 90 min the colored formazan product was solubilized with DMSO and the absorbance at 595 nm was measured.

Ex vivo murine retina angiogenesis (EMRA) assay

This assay was performed as described³⁸ using VEGF at 3.75 nM and lectins at 100 nM.

Ex vivo human artery ring assay

This assay was performed as described⁵⁹ using VEGF at 1.5 nM and lectins at 50 nM.

In vivo chick-embryo chorioallantoic membrane (CAM) assay

This assay was performed as described⁶⁰ using 100 ng VEGF in 3 µl and lectins at 50 nM.

Matrigel plug assay

Animal experiments were approved by our local animal ethics committee (OPBA) at the University of Brescia and were executed in accordance with national guidelines and regulations. Seven-week-old C57BL/6 female mice (Envigo, Bresso, Italy) were injected subcutaneously with 300 µl of liquid Matrigel containing 200 ng of FGF2 and 350 ng of VEGF in the absence or the presence of 70 µg of SNA or UEA. Matrigel with PBS alone was used as negative control. One week after injection, mice were sacrificed and plugs were harvested and processed for qRT-PCR as previously described.⁶¹

Statistical analysis

Data were reported as the mean ± s.e.m. Statistical analyses were performed using the statistical package Prism 6 (GraphPad Software). Data were analyzed with a one-way analysis of variance, and individual group comparisons were evaluated by the Bonferroni multiple comparison test or Student's *t*-test (matrigel plug assay). Differences were considered significant when *P* < 0.05. No sample was excluded from the analysis. The investigator was not blinded to group allocation when assessing results.

CONFLICT OF INTEREST

The authors declare no conflict of interest.

ACKNOWLEDGEMENTS

This work was supported by grant from Ministero dell'Istruzione, Università e Ricerca (MIUR) (ex 60%) to MR and by IG 18943 and MFAG 18459 grants from Associazione Italiana per la Ricerca sul Cancro (AIRC) to MP and RR, respectively. PC and SR were supported by AIRC Fellowships.

REFERENCES

1 Presta M, Dell'Era P, Mitola S, Moroni E, Ronca R, Rusnati M. Fibroblast growth factor/fibroblast growth factor receptor system in angiogenesis. *Cytokine Growth Factor Rev* 2005; **16**: 159–178.

2 Croci DO, Cerliani JP, Pinto NA, Morosi LG, Rabinovich GA. Regulatory role of glycans in the control of hypoxia-driven angiogenesis and sensitivity to anti-angiogenic treatment. *Glycobiology* 2014; **24**: 1283–1290.

3 Claesson-Welsh L, Welsh M. VEGFA and tumour angiogenesis. *J Intern Med* 2013; **273**: 114–127.

4 Ferrara N, Houck KA, Jakeman LB, Winer J, Leung DW. The vascular endothelial growth factor family of polypeptides. *Journal of Cellular Biochemistry* 1991; **47**: 211–218.

5 Hutchings H, Ortega N, Plouet J. Extracellular matrix-bound vascular endothelial growth factor promotes endothelial cell adhesion, migration, and survival through integrin ligation. *Faseb J* 2003; **17**: 1520–1522.

6 Fuh G, Garcia KC, de Vos AM. The interaction of neuropilin-1 with vascular endothelial growth factor and its receptor flt-1. *J Biol Chem* 2000; **275**: 26690–26695.

7 Koch S, Claesson-Welsh L. Signal transduction by vascular endothelial growth factor receptors. *Cold Spring Harbor Perspect Med* 2012; **2**: a006502.

8 Tao Q, Backer MV, Backer JM, Terman BI. Kinase insert domain receptor (KDR) extracellular immunoglobulin-like domains 4–7 contain structural features that block receptor dimerization and vascular endothelial growth factor-induced signaling. *J Biol Chem* 2001; **276**: 21916–21923.

9 Rahimi N, Costello CE. Emerging roles of post-translational modifications in signal transduction and angiogenesis. *Proteomics* 2015; **15**: 300–309.

10 Nacev BA, Grassi P, Dell A, Haslam SM, Liu JO. The antifungal drug itraconazole inhibits vascular endothelial growth factor receptor 2 (VEGFR2) glycosylation, trafficking, and signaling in endothelial cells. *J Biol Chem* 2011; **286**: 44045–44056.

11 Takahashi T, Shibuya M. The 230 kDa mature form of KDR/Flk-1 (VEGF receptor-2) activates the PLC-gamma pathway and partially induces mitotic signals in NIH3T3 fibroblasts. *Oncogene* 1997; **14**: 2079–2089.

12 Chuang IC, Yang CM, Song TY, Yang NC, Hu ML. The anti-angiogenic action of 2-deoxyglucose involves attenuation of VEGFR2 signaling and MMP-2 expression in HUVECs. *Life Sci* 2015; **139**: 52–61.

13 Markowska AI, Jefferies KC, Panjwani N. Galectin-3 protein modulates cell surface expression and activation of vascular endothelial growth factor receptor 2 in human endothelial cells. *J Biol Chem* 2011; **286**: 29913–29921.

14 Croci DO, Cerliani JP, Dalotto-Moreno T, Mendez-Huergo SP, Mascanfroni ID, Dergan-Dylon S et al. Glycosylation-dependent lectin-receptor interactions preserve angiogenesis in anti-VEGF refractory tumors. *Cell* 2014; **156**: 744–758.

15 Schauer R. Sialic acids as regulators of molecular and cellular interactions. *Curr Opin Struct Biol* 2009; **19**: 507–514.

16 Born GV, Palinski W. Unusually high concentrations of sialic acids on the surface of vascular endothelia. *Br J Exp Pathol* 1985; **66**: 543–549.

17 Cioffi DL, Pandey S, Alvarez DF, Cioffi EA. Terminal sialic acids are an important determinant of pulmonary endothelial barrier integrity. *Am J Physiol Lung Cell Mol Physiol* 2012; **302**: L1067–L1077.

18 Henry CB, DeFouw DO. Distribution of anionic sites on microvascular endothelium of the chick chorioallantoic membrane. *Tissue Cell* 1996; **28**: 449–454.

19 Kitazume S, Imamaki R, Kurimoto A, Ogawa K, Kato M, Yamaguchi Y et al. Interaction of platelet endothelial cell adhesion molecule (PECAM) with alpha2,6-sialylated glycan regulates its cell surface residency and anti-apoptotic role. *J Biol Chem* 2014; **289**: 27604–27613.

20 Chiodelli P, Urbinati C, Mitola S, Tanghetti E, Rusnati M. Sialic acid associated with alphavbeta3 integrin mediates HIV-1 Tat protein interaction and endothelial cell proangiogenic activation. *J Biol Chem* 2012; **287**: 20456–20466.

21 Chen JY, Tang YA, Huang SM, Juan HF, Wu LW, Sun YC et al. A novel sialyltransferase inhibitor suppresses FAK/paxillin signaling and cancer angiogenesis and metastasis pathways. *Cancer Res* 2011; **71**: 473–483.

22 Fairbrother WJ, Champe MA, Christinger HW, Keyt BA, Starovasnik MA. Solution structure of the heparin-binding domain of vascular endothelial growth factor. *Structure* 1998; **6**: 637–648.

23 Miyagawa S, Takeishi S, Yamamoto A, Ikeda K, Matsunari H, Yamada M et al. Survey of glycoantigens in cells from alpha1-3galactosyltransferase knockout pig using a lectin microarray. *Xenotransplantation* 2010; **17**: 61–70.

24 Safina G. Application of surface plasmon resonance for the detection of carbohydrates, glycoconjugates, and measurement of the carbohydrate-specific interactions: a comparison with conventional analytical techniques. A critical review. *Anal Chim Acta* 2012; **712**: 9–29.

25 Manning JC, Seyrek K, Kaltner H, Andre S, Sinowatz F, Gabius HJ. Glycomic profiling of developmental changes in bovine testis by lectin histochemistry and further analysis of the most prominent alteration on the level of the glycoproteome by lectin blotting and lectin affinity chromatography. *Histol Histopathol* 2004; **19**: 1043–1060.

26 Tatsuzuki A, Ezaki T, Makino Y, Matsuda Y, Ohta H. Characterization of the sugar chain expression of normal term human placental villi using lectin histochemistry combined with immunohistochemistry. *Arch Histol Cytol* 2009; **72**: 35–49.

27 Shibuya N, Goldstein IJ, Broekaert WF, Nsimba-Lubaki M, Peeters B, Peumans WJ. The elderberry (*Sambucus nigra* L.) bark lectin recognizes the Neu5Ac(alpha 2-6) Gal/GalNAc sequence. *J Biol Chem* 1987; **262**: 1596–1601.

28 Wang WC, Cummings RD. The immobilized leukoagglutinin from the seeds of *Maackia amurensis* binds with high affinity to complex-type Asn-linked oligosaccharides containing terminal sialic acid-linked alpha-2,3 to penultimate galactose residues. *J Biol Chem* 1988; **263**: 4576–4585.

29 Marino K, Bones J, Kattla JJ, Rudd PM. A systematic approach to protein glycosylation analysis: a path through the maze. *Nat Chem Biol* 2010; **6**: 713–723.

30 Chiodelli P, Mitola S, Ravelli C, Oreste P, Rusnati M, Presta M. Heparan sulfate proteoglycans mediate the angiogenic activity of the vascular endothelial growth factor receptor-2 agonist gremlin. *Arterioscler Thromb Vasc Biol* 2011; **31**: e116–e127.

31 Ravelli C, Mitola S, Corsini M, Presta M. Involvement of alphavbeta3 integrin in gremlin-induced angiogenesis. *Angiogenesis* 2013; **16**: 235–243.

32 Liu WS, Heckman CA. The sevenfold way of PKC regulation. *Cell Signal* 1998; **10**: 529–542.

33 Lauder H, Frost EE, Hiley CR, Fan TP. Quantification of the repair process involved in the repair of a cell monolayer using an in vitro model of mechanical injury. *Angiogenesis* 1998; **2**: 67–80.

34 Peverali FA, Mandriota SJ, Ciana P, Marelli R, Quax P, Rifkin DB et al. Tumor cells secrete an angiogenic factor that stimulates basic fibroblast growth factor and urokinase expression in vascular endothelial cells. *J Cell Physiol* 1994; **161**: 1–14.

35 Harduin-Lepers A, Vallejo-Ruiz V, Krzewinski-Recchi MA, Samyn-Petit B, Julien S, Delannoy P. The human sialyltransferase family. *Biochimie* 2001; **83**: 727–737.

36 Monaco L, Marc A, Eon-Duval A, Acerbis G, Distefano G, Lamotte D et al. Genetic engineering of alpha2,6-sialyltransferase in recombinant CHO cells and its effects on the sialylation of recombinant interferon-gamma. *Cytotechnology* 1996; **22**: 197–203.

37 Esko JD. Genetic analysis of proteoglycan structure, function and metabolism. *Curr Opin Cell Biol* 1991; **3**: 805–816.

38 Rezzola S, Belleri M, Ribatti D, Costagliola C, Presta M, Semeraro F. A novel ex vivo murine retina angiogenesis (EMRA) assay. *Exp Eye Res* 2013; **112**: 51–56.

39 Ribatti D. Chicken chorioallantoic membrane angiogenesis model. *Methods Mol Biol* 2012; **843**: 47–57.

40 Roskoski R Jr. VEGF receptor protein-tyrosine kinases: structure and regulation. *Biochem Biophys Res Commun* 2008; **375**: 287–291.

41 Leppanen VM, Prota AE, Jeltsch M, Anisimov A, Kalkkinen N, Strandin T et al. Structural determinants of growth factor binding and specificity by VEGF receptor 2. *Proc Natl Acad Sci USA* 2010; **107**: 2425–2430.

42 Brozzo MS, Bjelic S, Kisko K, Schleier T, Leppanen VM, Alitalo K et al. Thermodynamic and structural description of allosterically regulated VEGFR-2 dimerization. *Blood* 2012; **119**: 1781–1788.

43 Chandler KB, Leon DR, Meyer RD, Rahimi N, Costello CE. Site-specific N-glycosylation of endothelial cell receptor tyrosine kinase VEGFR-2. *J Proteome Res* 2017; **16**: 677–688.

44 Lee Jr J, Chen CH, Chen YH, Huang MJ, Huang J, Hung JS et al. COSMC is overexpressed in proliferating infantile hemangioma and enhances endothelial cell growth via VEGFR2. *PLoS One* 2013; **8**: e56211.

45 Franklin MC, Navarro EC, Wang Y, Patel S, Singh P, Zhang Y et al. The structural basis for the function of two anti-VEGF receptor 2 antibodies. *Structure* 2011; **19**: 1097–1107.

46 Cabral MG, Piteira AR, Silva Z, Ligeiro D, Brossmer R, Videira PA. Human dendritic cells contain cell surface sialyltransferase activity. *Immunol Lett* 2010; **131**: 89–96.

47 Taatjes DJ, Roth J, Weinstein J, Paulson JC. Post-Golgi apparatus localization and regional expression of rat intestinal sialyltransferase detected by immunoelectron microscopy with polypeptide epitope-purified antibody. *J Biol Chem* 1988; **263**: 6302–6309.

48 Garcia-Vallejo JJ, Van Dijk W, Van Het Hof B, Van Die I, Engelse MA, Van Hinsbergh VW et al. Activation of human endothelial cells by tumor necrosis factor-alpha results in profound changes in the expression of glycosylation-related genes. *J Cell Physiol* 2006; **206**: 203–210.

- 49 Abe Y, Smith CW, Katkin JP, Thurmon LM, Xu X, Mendoza LH *et al*. Endothelial alpha 2,6-linked sialic acid inhibits VCAM-1-dependent adhesion under flow conditions. *J Immunol* 1999; **163**: 2867–2876.
- 50 Lee C, Liu A, Miranda-Ribera A, Hyun SW, Lillehoj EP, Cross AS *et al*. NEU1 sialidase regulates the sialylation state of CD31 and disrupts CD31-driven capillary-like tube formation in human lung microvascular endothelia. *J Biol Chem* 2014; **289**: 9121–9135.
- 51 Doiron AL, Kirkpatrick AP, Rinker KD. TGF-beta and TNF-a affect cell surface proteoglycan and sialic acid expression on vascular endothelial cells. *Biomed Sci Instrum* 2004; **40**: 331–336.
- 52 Deng X, Zhang J, Liu Y, Chen L, Yu C. TNF-alpha regulates the proteolytic degradation of ST6Gal-1 and endothelial cell-cell junctions through upregulating expression of BACE1. *Sci Rep* 2017; **7**: 40256.
- 53 Brambilla A, Lonati E, Milani C, Rizzo AM, Farina F, Botto L *et al*. Ischemic conditions and ss-secretase activation: The impact of membrane cholesterol enrichment as triggering factor in rat brain endothelial cells. *Int J Biochem Cell Biol* 2015; **69**: 95–104.
- 54 Cai J, Qi X, Kociok N, Skosyrski S, Emilio A, Ruan Q *et al*. beta-Secretase (BACE1) inhibition causes retinal pathology by vascular dysregulation and accumulation of age pigment. *EMBO Mol Med* 2012; **4**: 980–991.
- 55 Antony P, Rose M, Heidenreich A, Knuchel R, Gaisa NT, Dahl E. Epigenetic inactivation of ST6GAL1 in human bladder cancer. *BMC Cancer* 2014; **14**: 901.
- 56 Windwarder M, Yelland T, Djordjevic S, Altmann F. Detailed characterization of the O-linked glycosylation of the neuropilin-1 c/MAM-domain. *Glycoconj J* 2015; **33**: 387–397.
- 57 Bugatti A, Giagulli C, Urbinati C, Caccuri F, Chiodelli P, Oreste P *et al*. Molecular interaction studies of HIV-1 matrix protein p17 and heparin: identification of the heparin-binding motif of p17 as a target for the development of multitarget antagonists. *J Biol Chem* 2013; **288**: 1150–1161.
- 58 Stabile H, Mitola S, Moroni E, Belleri M, Nicoli S, Coltrini D *et al*. Bone morphogenic protein antagonist Drm/gremlin is a novel proangiogenic factor. *Blood* 2007; **109**: 1834–1840.
- 59 Mitola S, Moroni E, Ravelli C, Andres G, Belleri M, Presta M. Angiopoietin-1 mediates the proangiogenic activity of the bone morphogenic protein antagonist Drm. *Blood* 2008; **112**: 1154–1157.
- 60 Urbinati C, Bugatti A, Oreste P, Zoppetti G, Waltenberger J, Mitola S *et al*. Chemically sulfated Escherichia coli K5 polysaccharide derivatives as extracellular HIV-1 Tat protein antagonists. *FEBS Lett* 2004; **568**: 171–177.
- 61 Coltrini D, Di Salle E, Ronca R, Belleri M, Testini C, Presta M. Matrigel plug assay: evaluation of the angiogenic response by reverse transcription-quantitative PCR. *Angiogenesis* 2013; **16**: 469–477.

Supplementary Information accompanies this paper on the Oncogene website (<http://www.nature.com/onc>)